Department of Mechanical Engineering and Mechanics

Drexel University College of Engineering

Proceedings of the 2004 IEEE
International Conference on Robotics & Automation
New Orleans, LA • April 2004

Flying Insect Inspired Vision for Autonomous Aerial Robot Maneuvers in Near-Earth Environments

William E. Green, Paul Y. Oh, and Geoffrey Barrows
Drexel University, Philadelphia PA and Centeye Inc., Washington DC
Email: [weg22 and paul.yu.oh]@drexel.edu and geof@centeye.com

Abstract

Near-Earth environments are time consuming, labor intensive and possibly dangerous to safe guard. Accomplishing tasks like bomb detection, search-and-rescue and reconnaissance with aerial robots could save resources. This paper describes the adoption of insect behavior and flight patterns to devolop a MAV sensor suite. A prototype called CQAR: Closed Quarter Aerial Robot, which is capable of flying in and around buildings, through tunnels and in and out of caves will be used to validate the efficiency of such a method when equipped with optic flow microsensors.

1 Introduction

More often, missions like search-and-rescue, reconnaisance and inspection are being performed in near-Earth environments like caves and forests or in urban structures like tunnels and large buildings. Such environments are time consuming and labor intensive to patrol and hence applying robots to assist in missions has become an active research area in recent years [2]. Much of the research effort has revolved around ground robots [8], however oftentimes a robot capable of flying or hovering may be more effective. For example, flying provides observation from an elevated position. Also, flying is often faster than crawling over rock piles found in tunnels or caves. Aerial robots that can fly in near-Earth environments such as micro-air-vehicles (MAVs) are small enough to fit in a backpack. Conventional navigational sensors, which work effectively for ground-based robots, are too heavy and large for MAVs which typically can only carry up to a cubic inch of payload weighing a maximum of 0.5 pounds [4] [5]. Some sensors, like global positioning systems, though small and light, don't work indoors and in enclosed near-Earth environments like tunnels or caves. Likewise, while miniature cameras exist, varied illumination and the lack of visual landmarks like the horizon, make them unsuitable. The net effect is that small and light navigational sensor suites are required to fly in near-Earth environments.

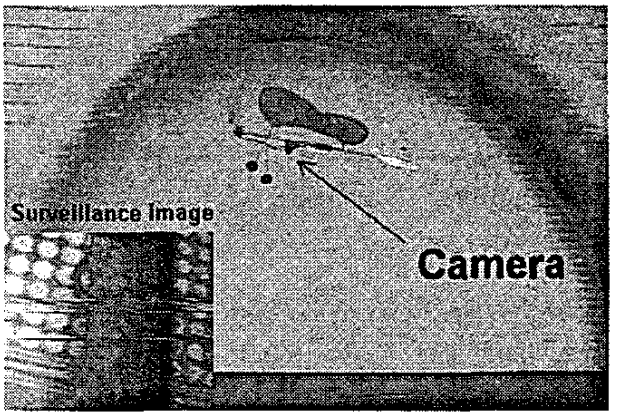

Figure 1: Our CQAR prototype can carry a 14 *gm* mini wireless camera and provide surveillance images (lower left shows a table) of urban structures.

Looking at [10], it is evident that flying insects, like honeybees, utilize optic flow to maneuver through regions with dense obstacle fields. Without GPS or IMUs, insects perform tasks like collision avoidance, altitude control, takeoff and landing and can therefore serve as a model for MAV flight patterns in such environments. Applying insect-inspired navigational methods to aerial robots is possible due to the development of optic flow microsensors weighing under 10 grams [1].

The evaluation of the suggested method requires an aerial testbed that can fly slowly for high maneuverability, is small enough to fit through narrow openings, and has a sufficient payload capacity. Figure 1 shows our protoype we call CQAR: *Closed Quarter Aerial Robot* (pronounced "seeker"). It weighs just 26 *grams* with a 45 *cm* wingspan and is capable of flying at cruise speeds less than 2 m/s (about the speed of a slow jogging person). Also, maintaining

0-7803-8232-3/04/$17.00 ©2004 IEEE

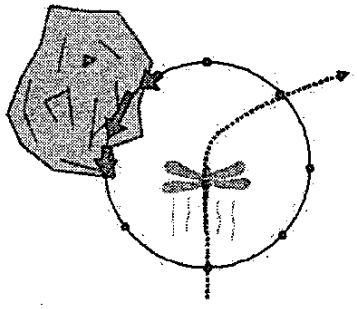

Figure 2: Dragon fly saccading away from regions of high optic flow in order to avoid a collision.

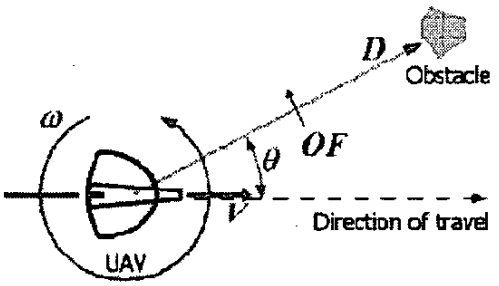

Figure 3: 1D optic flow during MAV flight.

steady level flight while carrying payloads as large as 15 *grams* is feasible [9]. This paper discusses an insect inspired aerial robot sensor suite as a lightweight and efficient solution for demonstrating autonomous tasks such as collision avoidance and automated landing in near-Earth environments. Section 2 discusses the theoretical background and the optic flow microsensors used to demonstrate such tasks. Section 3 describes the control system while section 4 refers to our future work in characterizing these microsensors. Finally, section 5 concludes by summarizing.

2 Optic Flow for Navigation

Insects make heavy use of vision, especially optic flow, for perceiving the environment [3]. Optic flow refers to the apparent movement of texture in the visual field relative to the insect's velocity. Insects perform a variety of tasks in complex environments by using their natural optic flow sensing capabilities. While in flight, for example, objects which are in close proximity to the insect have higher optic flow magnitudes. Thus, flying insects, such as fruit flies [11] and dragon flies, avoid imminent collisions by saccading (or turning) away from regions of high optic flow (see Figure 2). With optic flow sensors, efficient and robust navigational sensor suites for MAVs can be developed by mimicking the natural behaviors of insects.

2.1 From Insects to MAVs

Theoretically, optic flow is measured in *rad/sec* and is a function of the UAV's forward velocity, V, angular velocity, ω, distance D from an object, and the angle, θ, between the MAV's direction of travel and the object (see Figure 3).

$$OF = \frac{V}{D}\sin\theta - \omega \qquad (1)$$

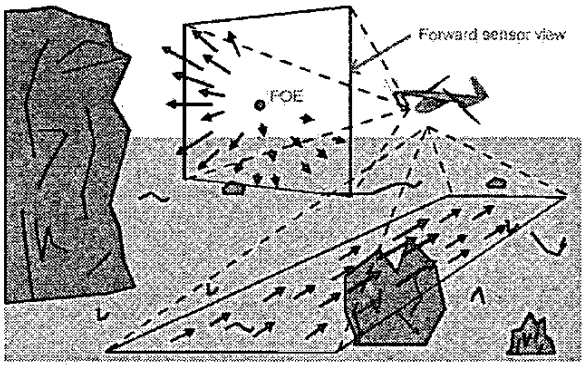

Figure 4: Optic flow as seen by aerial robot flying above ground.

Figure 4 depicts optic flow as it might be seen by a MAV traveling a straight line above the ground. The focus of expansion (FOE) in the forward sensor view indicates the direction of travel. If the FOE is located inside a rapidly diverging region, then a collision is imminent. A rapidly expanding region to the right of the FOE (like the one seen in the Figure 4) corresponds to an obstacle approaching on the right side of the MAV. Thus, the MAV should turn left, or away from the region of high optic flow, to avoid the collision. Similarly, the MAV can estimate its height from the optic flow in the downward direction; faster optic flow indicates a low flight altitude. By equiping a MAV with sensors capable of measuring the optic flow in front of and below the aircraft, the above flight patterns can be embedded in a sensor suite for autonomous navigation.

2.2 Microsensors

Nueromorphic chips have been available for many years [7]. However, to achieve the desired weight of 1-2 grams, mixed-mode and mixed-signal VLSI tech-

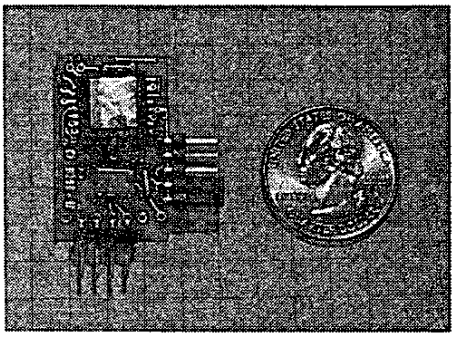

Figure 5: mixed-mode VLSI optic flow microsensor is slightly bigger than a US quarter.

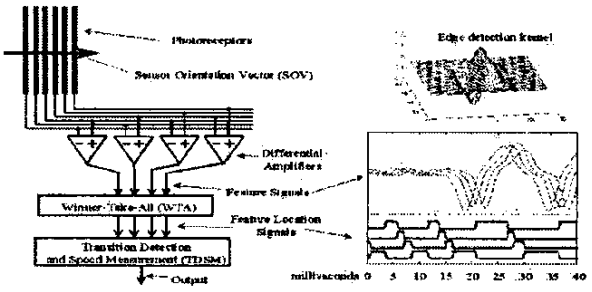

Figure 6: The feature tracker elementary motion detector (EMD).

niques are used to develop compact circuits that directly perform computations necessary to measure optic flow. Centeye has developed the one-dimensional *Ladybug* optic flow microsensor based on such techniques and is shown in Figure 5. These sensors are inspired by the general optic flow model of animal visual systems. A lens focuses an image of the environment onto a focal plane chip, which contains photoreceptor circuits and other circuits necessary to compute optic flow. Low level feature detectors respond to different spatial or temporal entities in the environment, such as edges, spots, or corners. The elementary motion detector (EMD) is the most basic structure or entity that senses visual motion, though its output may not be in a form easily used. Fusion circuitry fuses information from the EMDs to reduce errors, increase robustness, and produces a meaningful representation of the optic flow for specific applications.

Figure 6 depicts a simple realization of the feature tracker EMD algorithm used [1]. On the left is the basic EMD architecture, on the upper right is an edge detection kernel implemented by a differential amplifier, and on the lower right are sample traces of feature signals and feature location signals. This EMD measures one-dimensional optic flow in one part of the visual field, thus the complete sensor would have many such EMDs replicated throughout the visual field. Functionally there are four sections, as shown in Figure 6: photoreceptors, feature detectors (shown here as differential amplifiers), a winner-take-all (WTA), and a transition detection and speed measurement section (TDSM).

A section of the focal plane is sampled with an array of elongated rectangular photoreceptors laid out so that the array is positioned along the sensor orientation vector (SOV). The photoreceptor rectangles are arranged so that their long axes are perpendicular to the SOV. This layout filters out visual information perpendicular to the SOV direction while retaining information in the parallel direction. One effect of these rectangular photoreceptors is that the measurement of the sensor is actually a measurement of the projection of the two dimensional optic flow vector onto the SOV vector [1].

The outputs from the photoreceptors are sent to an array of four feature detectors that output four analog feature signals. A feature detector circuit attains its highest output value when the feature to which it is tuned appears on its input photoreceptors. For example, suppose the feature detectors are differential amplifiers. Then their effective response function is the edge detection kernel, shown in the upper right part of Figure 6. A feature signal will have a high value when an edge is located between the input photoreceptors with the brighter side on the positively connected photoreceptor.

The four analog feature signals are then sent to a winner-take-all (WTA). The WTA has four analog inputs and four digital outputs. The WTA determines which input has the highest value and sets the corresponding output a digital high (or 1), and all the other outputs low (or 0). The location of the high value indicates where on the photoreceptor array the image is most like the feature defined by the configuration vector. The WTA outputs are thus also called feature location signals. As an edge moves across the photoreceptors shown in Figure 6, the high value will move sequentially across the WTA outputs. This is easily visualized with the aid of the trace in the lower right part of Figure 6. Shown are four feature signals and their corresponding feature location signals when the photoreceptors are exposed to a moving black and white bar pattern.

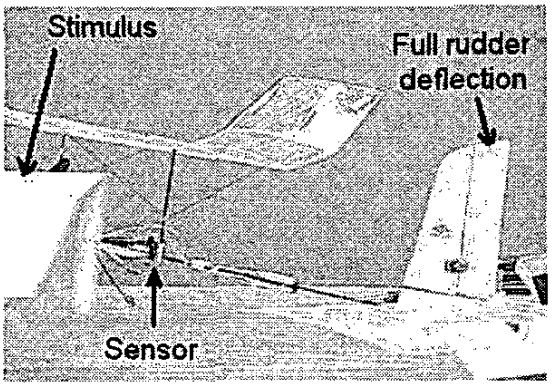

Figure 7: Contrast variation prompts full rudder deflection as a result of "bang bang" control.

The transition detection and speed measurement (TDSM) circuit converts the movement of the high WTA output into a velocity measurement. Essentially this circuit is a state machine that responds to the WTA outputs and interprets the 1-2-3-4 motions of the high feature location signal as visual motion. Whenever the high feature location signal moves in a manner that indicates visual motion, the EMD generates a measurement of the optic flow. The direction of the visual motion is determined by the direction of travel of the high feature location signal. Likewise the speed is obtained with the lag-time from one feature location to the next. This lag-time is also referred to as the transition interval. Then the actual optic flow can be determined from the physical geometry of the photoreceptor array and the sensor optics.

The resulting sensor, including optics, imaging, processing, and I/O weighs 4.8 grams. This sensor grabs frames up to 1.4 kHz, measures optic flow up to 20 rad/s (4 bit output), and functions even when texture contrast is just several percent (see Figure 7).

3 Autonomous Tasks

Optic flow microsensors can be oriented to perceive information about oncoming collisions and altitude. For example, positioning sensors such that the optical axis faces in the forward direction will allow the measurement of the optic flow field in front of the aircraft. Likewise, measuring the optic flow on the ground requires placing a sensor on the belly of the MAV. Such information can be used to mimic insect flight patterns to perform autonomous collision avoidance and landings for MAVs.

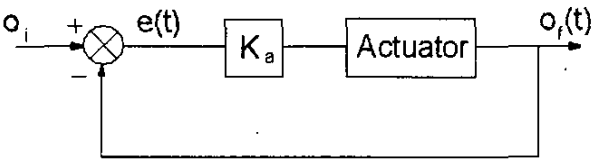

Figure 8: Optic flow control system block diagram.

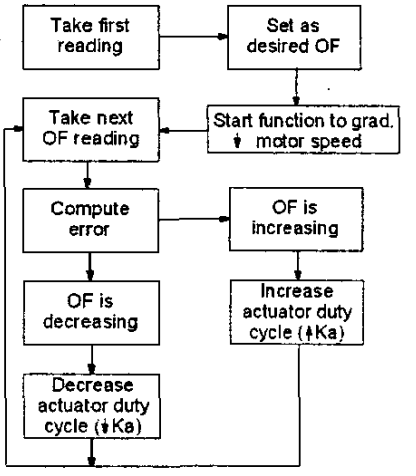

Figure 9: Flow chart of landing control system.

3.1 Landing

Srinivasan observed that honeybees land by keeping the optic flow on the landing surface constant. It is possible to autonomously land a MAV by mimicking this behavior [6]. When measuring the optic flow on the landing surface, the obstacle is now the ground and thus $\theta = 90$. To further simplify this task, the rotational component of optic flow arising from changes in aircraft pitch are assumed smaller than the translational component. Thus, equation (1) reduces to

$$OF = \frac{V}{D} \tag{2}$$

Keeping equation (2) constant (where D is the altitude) demands the aircraft's control system decrease forward speed in proportion to altitude.

The control system block diagram and flow chart are shown in Figures 8 and 9 respectively. When approaching a landing, an embedded microcontroller (see Figure 10), will implement a function to gradually throttle down the motor while continuing to take readings throughout the landing process. The error, $e(t)$, is computed between the desired optic flow, o_i

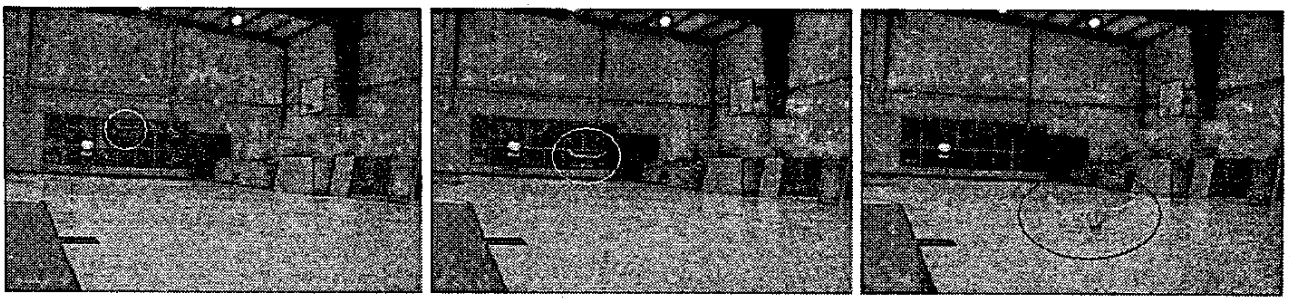

Figure 11: The optic flow on the basketball gym floor is kept constant by the control system. That is, the aircraft (encircled) forward velocity is decreased in proportion with its altitude to land smoothly. Left: Aircraft just after hand launch. Middle: Aircraft midway through landing sequence at proportionally lower altitude and velocity. Right: Aircraft comes to a smooth landing within 25 *meters* from starting point.

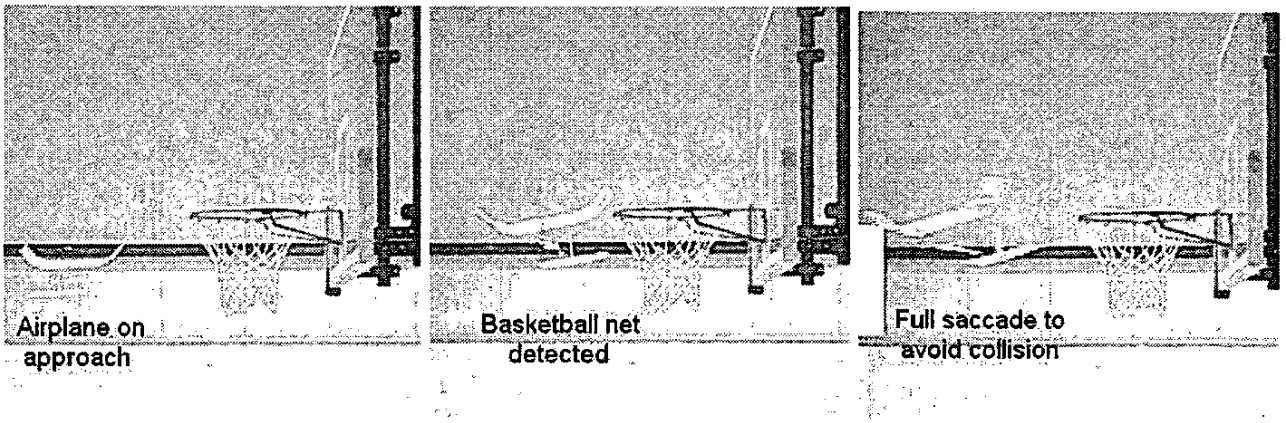

Figure 12: Optic flow is used to sense when an obstacle is within two turning radii of the aircraft. The aircraft avoids the collision by fully deflecting the rudder.

which was estimated beforehand, and the actual optic flow value, $o_f(t)$. When the optic flow on the landing surface becomes larger than the desired optic flow, the error is negative and two conditions are possible. One, the forward velocity, V, could be significantly increasing which is not possible based on the motor function. Two, the altitude, D, can be decreasing at a faster rate than V. Here, the controller will send a signal to the elevator to decrease the vehicle's descent rate based on the error magnitude and proportional constant, K_a. The other possibility is that the optic flow could start to dip below the desired level causing the error to be positive. The two possible cases that arise here are one, D is increasing but again this is not practical while in landing mode and two, V is decreasing faster than D. In this case, the controller will need to command the elevator to increase the descent rate. After a control sequence has been implemented to force the optic flow back to the desired value, the elevator resets to its neutral position. By implementing this control scheme, we were able to successfully demonstrate an autonomous landing (see Figure 11).

3.2 Collision Avoidance

MAVs can also turn away from regions of high optic flow in the same manner that insects do to avoid collisions in complex environments. Optic flow must be detected in front of the vehicle in order to avoid collisions and thus, the sensor must be positioned at some angle forward. Unlike with autonomous landing, where the sensor was oriented at 90 degrees to the direction of travel, the angle θ to the obstacle will be a factor. Assuming the MAV is traveling in a straight path with a relatively constant translational veloctiy, V, we have from equation 1

$$OF = \frac{V}{D}\sin\theta \tag{3}$$

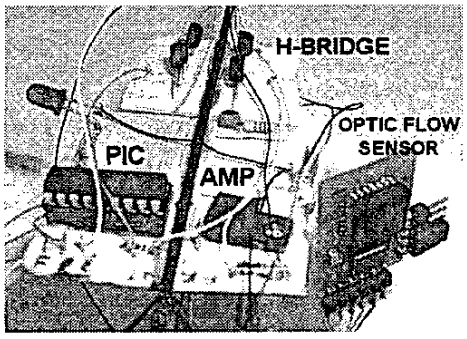

Figure 10: A microcontroller is used to read the digital output of the optic flow sensor and implement the control algorithms. The control signal is then sent through an H-bridge to deflect the aircraft's control surfaces.

An optic flow threshold was set to correspond to an obstacle being within two turning radii of the aircraft. Thus, when the threshold is exceeded, the sensor suite will implement proportional rudder control to safely avoid the obstacle. By implementing this method, autonomous collision avoidance was successfully demonstrated (see Figure 12).

4 Future Work

Optic flow sensors are sensitive to changing environmental conditions such as lighting levels, texture variation, and maximum detection distance. While such parameters can be generalized, the resulting control design is *ad hoc*. However, through sensor characterization, algorithms can be formulated and optimized.

Characterizing optic flow sensors requires a system such that the relative motion of a sensor and viewing target can be produced as often as desired and is repeatable to a few percent in relative velocity, viewing angle, viewing distance, target composition, and lighting conditions. Further, the target should be viewable at angles ranging from zero degrees (with the optical axis of the sensor pointing in the direction of travel) to ninety degrees (with optical axis perpendicular to direction of travel). Such sensor characterization will setup a framework upon which controllers can be analytically designed. This enables one to assess the performance of an autonomous MAV quantitatively.

5 Conclusions

Near-Earth environments which occlude conventional navigational methods, such as GPS satellites and the horizon, are time consuming and labor intensive to patrol and safekeep. Lightweight optic flow microsensors, based on the vision system of flying insects, are suitable for MAV payload capacities. This paper presented how such VLSI hardware can be utilized for MAV navigation. Furthermore, a closed quarter aerial robot (CQAR) prototype equipped with an optic flow sensor suite was able to demonstrate autonomous tasks such as collision avoidance and automated landings.

References

[1] Barrows, G., "Mixed-Mode VLSI Optic Flow Sensors for Micro Air Vehicles", *Ph.D. Dissertation*, University of Maryland, College Park, MD, Dec. 1999.

[2] Blitch, J., "World Trade Center Search-and-Rescue Robots", Plenary Session *IEEE Int Conf Robotics and Automation*, Washington D.C., May 2002.

[3] Gibson, J.J., *The Ecological Approach to Visual Perception*, Houghton Mifflin, 1950.

[4] Grasmeyer, J.M., Keennon, M.T., "Development of the Black Widow Micro Air Vehicle", *39th AIAA Aerospace Sciences Meeting and Exhibit*, Reno, NV, Jan. 2001.

[5] Green, W.E., Oh, P.Y., "An Aerial Robot Prototype for Situational Awareness in Closed Quarters", *IEEE/RSJ Int Conf on Intelligent Robots and Systems*, pp. 61-66, Las Vegas, NV, Oct. 2003.

[6] Green, W.E., Oh, P.Y., Barrows, G., Sevcik, K., "Autonomous Landing for Indoor Flying Robots Using Optic Flow", *ASME Int. Mech. Eng. Congress and Expo.*, v2, pp. 1341-1346, Wash., D.C., Nov. 2003.

[7] Netter, T., Francheschini, N., "A Robotic Aircraft that Follows Terrain Using a Neuromorphic Eye", *IEEE/RSJ Int Conf on Intelligent Robots and Systems*, V1, pp. 129-134, Lausanne, Switz., Sept. 2002.

[8] Murphy, R., et al, "Mobility and sensing demands in USAR", *IEEE Industrial Electronics Conference (IECON)*, V1, pp. 138-142, 2000.

[9] Oh, P.Y., Green, W.E., "Closed Quarter Aerial Robot Prototype to Fly In and Around Buildings", *Int. Conference on Computer, Communication and Control Technologies*, Vol. 5, pp. 302-307, Orlando, FL, July 2003.

[10] Srinivasan, M.V., Chahl, J.S., Weber, K., Venkatesh, S., Nagle, M.G., Zhang, S.W., *Robot Navigation Inspired By Principles of Insect Vision* in Field and Service Robotics, A. Zelinsky (ed), Springer Verlag Berlin, NY 12-16.

[11] Tammero, L.F., Dickinson, M.H., "The influence of visual landscape on the free flight behavior of the fruit fly Drosophila melanogaster", *Journal of Experimental Biology*, v205, pp. 327-343, 2002.